Ligand and Substituent Effects on the Dynamics and Structure of Agostic Complexes of the Type $C_5R_5(L)Co(CH_2CHR'\text{-}\mu\text{-}H)^+BF_4^-$ (L = $P(OMe)_3$, PMe_3; R = H, Me; R' = H, Me)

M. Brookhart,* D. M. Lincoln, A. F. Volpe Jr., and Gregory F. Schmidt

Department of Chemistry, The University of North Carolina, Chapel Hill, North Carolina 27599

Received August 31, 1988

Protonation of ethylene complexes $C_5R_5(L)Co(CH_2CH_2)$ with $HBF_4{\cdot}OMe_2$ in CD_2Cl_2 gives agostic complexes $C_5R_5(L)Co\text{-}CH_2CH_2\text{-}\mu\text{-}H^+$ (R = CH_3, **4a**, L = PMe_3, **4b**, L = $P(OMe)_3$; R = H, **5a**, L = PMe_3, **4b**, L = $P(OMe)_3$). ^1H and ^{13}C NMR spectra of the static structures at −70 °C establish three-center, two-electron Co···H_a···C bonding. Species **4a,b** and **5a,b** undergo three degenerate dynamic processes. Free energies of activation for these processes were measured by variable-temperature ^1H and ^{13}C NMR spectroscopy. Process I is rotation of the agostic methyl group. The $\Delta G^{\ddagger}$'s for process I are independent of L but 1.5 kcal/mol less for Cp* relative to Cp. Process II involves rotation of the C_2 fragment via intermediacy of the classical ethylene hydride complex. Inversion at the Co center via a 16-electron alkyl species accounts for process III. Protonation of $C_5Me_5(P(OMe)_3)Co(CH_2CHCH_3)$ leads to three methyl-substituted isomers, the two major ones possessing the methyl substituent at C_β and a minor one with the methyl substituent at C_α. The unusual spectral properties of the major isomer (J_{CH_a} = 38.5 Hz, J_{PH_a} = 39 Hz) suggest either nearly equally populated agostic and classical hydride forms which rapidly interconvert *or* a complex whose static structure is intermediate between a classical hydride (J_{CH} = ca. 0 Hz, J_{PH} = ca. 80 Hz) and a "normal" agostic structure (J_{CH_a} = 60 Hz, J_{PH_a} = 12 Hz).

Introduction

Several mononuclear transition-metal complexes containing agostic ethyl groups (general structure **1**) are now known[1] including $(dmpe)(Cl)_3Ti(C_2H_4\text{-}\mu\text{-}H)$,[2] $(PMe_3)_2(Cl)_2(Me_3CCH)Ta(CH_2CH_2\text{-}\mu\text{-}H)$,[3] $Cp^*_2Sc(CH_2CH_2\text{-}\mu\text{-}H)$,[4] $Cp(CO)_2W(CH_2CH_2\text{-}\mu\text{-}H)$,[5,6] $(\eta^3\text{-}C_3H_5)_3Mo(CH_2CHR\text{-}\mu\text{-}H)$,[7] and $Cp^*(L)Co(CH_2CH_2\text{-}\mu\text{-}H)^+$ where L = C_2H_4,[8] P(*p*-tolyl)$_3$,[9] PMe_3,[9,10] $PPhMe_2$,[11] and $P(OMe)_3$.[10,12] Closely related species include the agostic complexes formed from protonation of (norbornadiene)tricarbonyliron,[1,13] (dicyclopentadiene)ML_n (ML_n = RuC_6Me_3, $OsMe_3H_3$, RhC_5Me_5, and IrC_5Me_5),[14] and $(R_2P\text{-}(CH_2)_n\text{-}PR_2)Pt$(norbornene).[15] NMR spectroscopic studies have established that for most systems the agostic ethyl species **1** is in rapid equilibrium with the unsaturated alkyl complex **2**[1-12] and, in certain cases, the terminal ethylene hydride species **3**.[8-13,15]

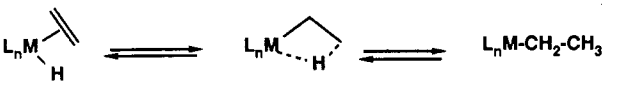

3 **1** **2**

Table I. Selected ^1H and ^{13}C NMR Data for 4a,b and 5a,b

compd[a]	H_a	C_α	C_β	J_{CH_a}, Hz
4a	−12.6	25.8	−4.7	63
4b	−12.1	26.5	−5.8	61
5a	−13.0	20.4	−9.6	60
5b	−12.4	22.0	−9.2	61

[a] All spectra recorded at −70 °C in CD_2Cl_2 with the exception of ^{13}C data for **4b** which was recorded at −90 °C. Chemical shifts are in ppm relative to TMS taken as 0 ppm.

Of particular interest to us are cobalt systems of the type shown below generated from protonation of the ethylene complexes $C_5R_5(L)Co(C_2H_4)$ (L = C_2H_4, PR_3, $P(OR)_3$).[8-12]

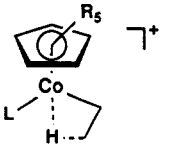

L = C_2H_4, PR_3, $P(OR)_3$
R = Me, H

Certain of these species are ethylene polymerization catalysts that form living polymers.[9,10,12] We have proposed[12] that the existence of an agostic M···H···C bridge in these complexes suggests that alkyl migrations in the analogous alkyl olefin complexes should be facile. Thus, efficient olefin polymerization can occur via the sequence shown in Scheme I.

The variation of the dynamics and structure of these cobalt complexes with ligand and alkene structure is im-

(1) (a) Brookhart, M.; Green, M. L. H.; Wong, L.-L. *Prog. Inorg. Chem.* **1988**, *36*, 1-124. (b) Brookhart, M.; Green, M. L. H. *J. Organomet. Chem.* **1983**, *250*, 395.
(2) (a) Dawoodi, Z.; Green, M. L. H.; Mtetwa, U. S. B.; Prout, K. *J. Chem. Soc., Chem. Commun.* **1982**, 802. (b) Dawoodi, Z.; Green, M. L. H.; Mtetwa, U. S. B.; Prout, K.; Schultz, A. J.; Williams, J. M.; Koetzle, T. F. *J. Chem. Soc., Dalton Trans.* **1986**, 1629.
(3) Fellmann, J. D.; Schrock, R. R.; Trificante, D. D. *Organometallics* **1982**, 1, 481.
(4) Thompson, M. E.; Baxter, S. M.; Bulls, A. R.; Burger, B. J.; Nolan, M. C.; Santarsiero, B. D.; Schaefer, W. P.; Bercaw, J. E. *J. Am. Chem. Soc.* **1987**, *109*, 203.
(5) Kazlavskas, R. J.; Wrighton, M. S. *J. Am. Chem. Soc.* **1982**, *104*, 6005.
(6) Yang, G. K.; Peters, K. S.; Vaida, V. *J. Am. Chem. Soc.* **1986**, *108*, 2511.
(7) Benn, R.; Holle, S.; Jolly, P. W.; Mynott, R.; Romao, C. C. *Angew. Chem., Int. Ed. Engl.* **1986**, *25*, 556.
(8) Brookhart, M.; Green, M. L. H.; Pardy, R. B. A. *J. Chem. Soc., Chem. Commun.* **1983**, 691.
(9) Cracknell, R. B.; Orpen, A. G.; Spencer, J. L. *J. Chem. Soc., Chem. Commun.* **1984**, 326.
(10) Brookhart, M.; Schmidt, G. F.; Lincoln, D.; Rivers, D. Olefin Insertion Reactions: The Mechanism of Co(III) Catalyzed Polymerization. In *Transition Metal Catalyzed Polymerization: Ziegler-Natta and Metathesis Polymerization*; Quirk, R. P., Ed.; Cambridge Press: Oxford, 1988.
(11) Cracknell, R. B.; Orpen, A. G.; Spencer, J. L. *J. Chem. Soc., Chem. Commun.* **1986**, 1005.
(12) Schmidt, G. F.; Brookhart, M. *J. Am. Chem. Soc.* **1985**, *107*, 1443.
(13) Olah, G. A.; Yu, S. H.; Liang, G. *J. Org. Chem.* **1976**, *41*, 2383.
(14) Bennett, M. A.; McMahon, I. J.; Pelling, S.; Robertson, G. B.; Wickramasinghe, W. A. *Organometallics* **1985**, *4*, 754.
(15) Carr, N.; Dunne, B. J.; Orpen, G. A.; Spencer, J. L. *J. Chem. Soc., Chem. Commun.* **1988**, 926.

0276-7333/89/2308-1212$01.50/0

Scheme I

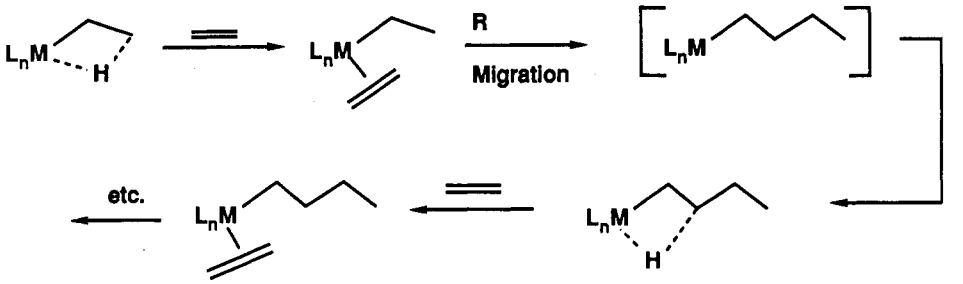

portant not only for a fundamental understanding of the energetic relationships between the agostic species **1** and the classical ethylene hydride and 16-electron alkyl forms **2** and **3** but also in making connections between the properties of these agostic species and their characteristics as olefin polymerization catalysts.

We report here (1) a spectroscopic study of the structure and dynamics of $C_5H_5(L)Co\text{-}CH_2CH_2\text{-}\mu\text{-}H^+$ (**5a**, L = PMe_3, **5b**, L = $P(OMe)_3$) together with a comparison to $C_5Me_5(L)Co\text{-}CH_2CH_2\text{-}\mu\text{-}H^+$ (**4a**, L = PMe_3,[9] **4b**, L = $P(OMe)_3$[12]) and (2) the structure and dynamics of the agostic methyl-substituted system $C_5Me_5(P(OMe)_3)Co\text{-}C_2H_3(CH_3)\text{-}\mu\text{-}H^+$. Systems **4a** and **4b** have been previously identified as agostic systems by Spencer[9] and ourselves,[12] respectively, but only partial NMR and dynamic data are available.

Results and Discussion

A. Generation and Spectroscopic Characterization of Static $C_5Me_5(L)Co\text{-}CH_2CH_2\text{-}\mu\text{-}H^+$ (4a,b) and $C_5H_5(L)Co\text{-}CH_2CH_2\text{-}\mu\text{-}H^+$ (5a,b) (a, L = PMe_3, b, L = $P(OMe)_3$). The agostic species **4a,b** and **5a,b** were generated for NMR spectroscopic observation by protonation of the neutral ethylene complexes **6** and **7** with $Me_2O\cdot HBF_4$ in CD_2Cl_2 at −30 °C. Static ^1H and ^{13}C spectra of these

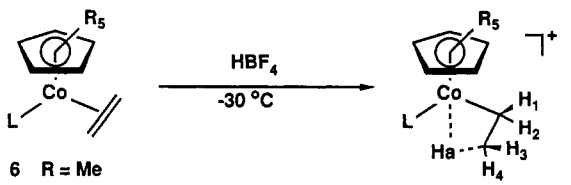

6 R = Me
7 R = H
L = (a) PMe_3 (b) $P(OMe)_3$

4 R = Me
5 R = H

species were recorded below −70 °C, and key parameters are summarized in Table I. Complete spectroscopic data are given in the Experimental Section. Definitive evidence for an agostic interaction comes from the reduced values of $J_{C_\beta\text{-}H_a}$ of 60–63 Hz.[1] Also indicative of M···H···C interactions in these complexes are the high-field shifts of both C_β (−5 to −9 ppm) and the bridging hydrogen H_a (−12 to −13 ppm). The J_{PH_a} values in **4a,b** and **5a,b** are estimated as ca. 12 Hz.[16] These values can be compared to J_{PH} = 80 Hz in $C_5Me_5(P(OMe)_3)_2Co\text{-}H^+$ which serves as a model for J_{PH} in a classical, terminal hydride structure.[17] Such low J_{PH_a} couplings have been noted in other agostic species involving phosphine and phosphite complexes and are a further indication of a reduced Co–H bond order in the 3c–2e Co···H···C bond.[1]

Ground-state structures of **4a,b** and **5a,b**, are quite similar as judged by spectral data. All $J_{C\text{-}H_a}$'s fall in a narrow range (60–63 Hz) as do the δ values (−12.1 to −13.0 ppm). The C_β shifts are ca. 5 ppm to higher fields in the Cp relative to Cp* derivatives which could imply slightly enhanced Co–C_β interactions, but this is not reflected in any other spectral features.

Table II. Free Energies of Activation for Dynamic Processes I, II, and III[a]

compd	process I[b]	process II[c]	process III
4a	10.9	>15.6	13.4[d]
4b	11.1	13.4	*e*
5a	12.5	13.4	*e*
5b	12.5	12.7	*e*

[a] Values in kcal/mol; error limits ca. 0.2 kcal/mol. [b] Determined from line broadening of H_a in slow-exchange region. [c] Determined from line broadening of $^{13}C_\alpha$, $^{13}C_\beta$ in slow-exchange region. [d] Determined by line broadening of H_1, H_2 in slow-exchange region. [e] Masked by processes I and II; see text.

B. Dynamic Processes in 4a,b and 5a,b. Summarized below are three dynamic processes which agostic ethyl species **4a,b** and **5a,b** exhibit. Process I results in site

Process I: Agostic Methyl Rotation

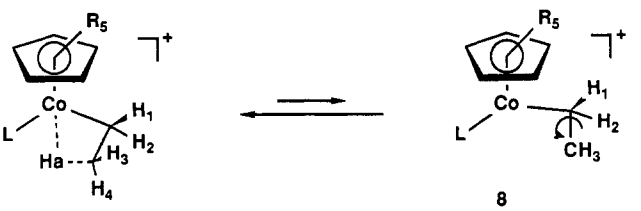

8

exchange of H_a, H_3, and H_4 and could occur via 16-electron species **8** or by methyl rotation within the agostic species such that the CH_3 group always retains some interaction with the cobalt center. Such an "in place" methyl rotation has recently been proposed to account for a similar dynamic process in a molybdenum ethylene hydride complex.[18] Process I results in NMR line broadening of H_a, H_3, and H_4, but since process II can also broaden H_3 and H_4, the most reliable way to estimate this barrier is via measurement of line broadening of H_a in the slow-exchange limit. Process I is the only process that results in site exchange of H_a. Process II is interpreted as occurring via formation of classical hydride **9** followed by ethylene rotation and rebridging. The measured $\Delta G^\ddagger$ will be composed of $\Delta G_{eq} + \Delta G^\ddagger_{rot}$. This process alone interchanges H_2 with H_3 and H_1 with H_4. However, coupled with the normally faster process I, exchange of all five hydrogens H_a and H_1–H_4 occurs. This is the only process which results in exchange of C_α with C_β; hence the most reliable method for measuring the barrier is by line-width analysis

(16) Decoupling experiments on **4b** establish that H_a is coupled to the β protons at δ −0.2 and −0.3 ppm by 12 and 20 Hz, respectively, and by less than ca. 5 Hz to the α protons (δ 1.9 and 2.5 ppm). The remaining 12 Hz coupling is thus assigned to the J_{PH}. Since the signal pattern of H_a is very similar for **4a,b** and **5a,b**, we assume that all J_{PH} values for these species are ca. 12 Hz.

(17) Volpe, A.; Brookhart, M., unpublished results.

(18) Green, M. L. H.; Wong, L.-L. *J. Chem. Soc., Chem. Commun.* 1988, 677.

Process II: Ethylene Rotation

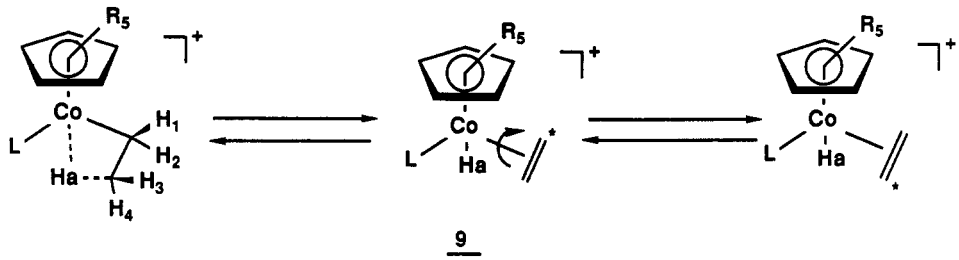

9

Chart I

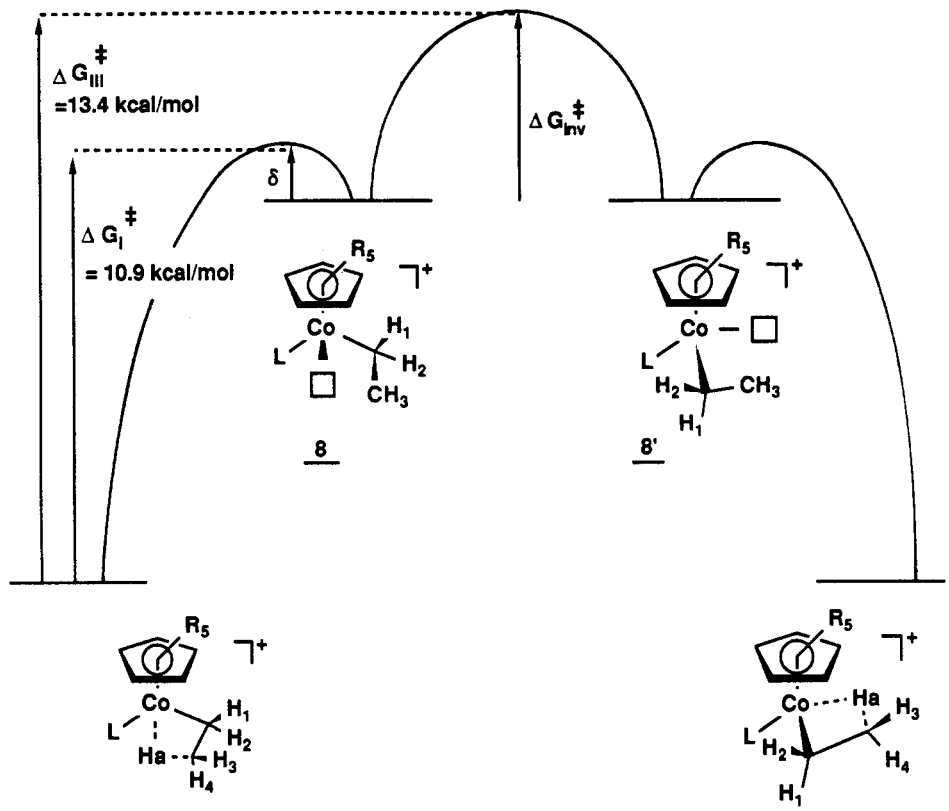

8 8'

of C_α and C_β under slow exchange conditions. The cobalt inversion process most likely occurs as illustrated above. Cleavage of the agostic CH···Co bond results in formation of 16-electron species 8, an octahedral complex containing a vacant coordination site. Cobalt inversion occurs at this stage followed by collapse back to 4.

This isomerization can be spectroscopically detected only in certain systems. When process III is *faster* than process II, $\Delta G^{\ddagger}_{III}$ can be measured by using line broadening of H_1, H_2 which are exchanged via this mechanism. However, when $k_{III} < k_{II}, k_I$ (the usual case), five-hydrogen scrambing via process II coupled with process I masks process III. Spencer[11] has used a clever technique for determining k_{III} which involves measuring the rate of exchange of diastereotopic methyl groups in **10**. The *only* mechanism that averages methyls in **10** is inversion at cobalt.

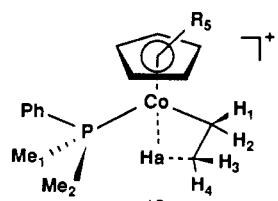

10

The dynamic processes described above were measured as indicated for species **4a,b** and **5a,b** and are summarized in Table II. Only for complex **5a** was the rate of process III detectable since in this case $k_{III} > k_{II}$.

A surprising observation is that the methyl rotational barrier is insensitive to the nature of the phosphine ligand (PMe_3 vs $P(OMe)_3$) in both the Cp and Cp* series. The barrier is slightly sensitive to Cp vs Cp* with $\Delta G^{\ddagger}$'s ca. 1.5 kcal/mol higher for Cp analogues. The reasons for these trends are not apparent. The difference in the Cp* vs Cp barriers is consistent with an electronic effect. The energy difference between electron-deficient **8** and the 18-electron agostic species **4** is expected to be higher for Cp than the better donor Cp*. This explanation seems inconsistent with the barrier insensitivity to L. However, it should be noted that L is cis while Cp/Cp* is trans to the agostic H and so electronic effects could differ substantially for L and Cp/Cp*. If "in place" methyl rotation occurs and no true 16-electron species is formed,[18] electronic effects could be small and thus this mechanism would be consistent with the data.

The cobalt inversion barrier of 13.4 kcal/mol is similar to the barrier of 13.4 ± 1 kcal/mol reported by Spencer[11] for **10**. If the process occurs as shown above, the free energy diagram must look approximately as shown in

Process III: Inversion at Cobalt

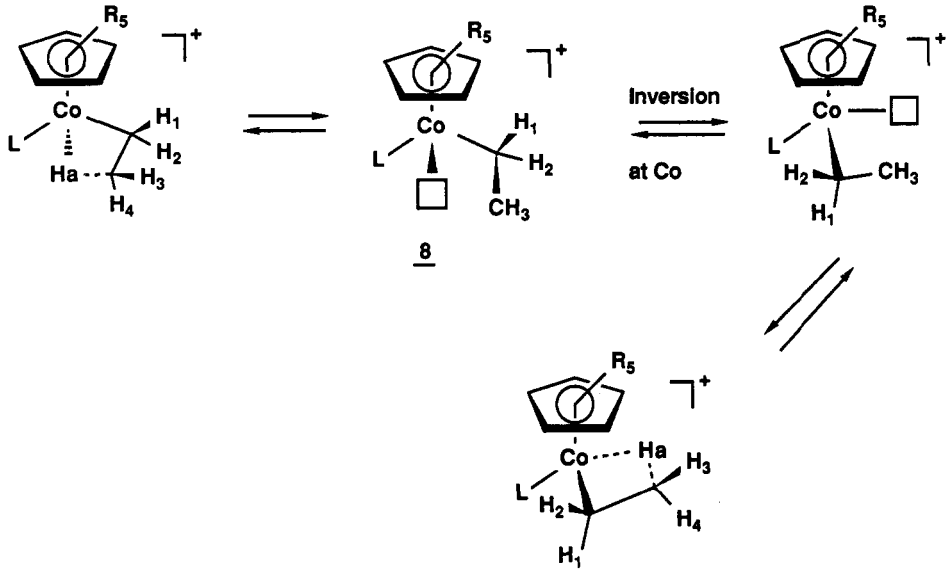

Chart II

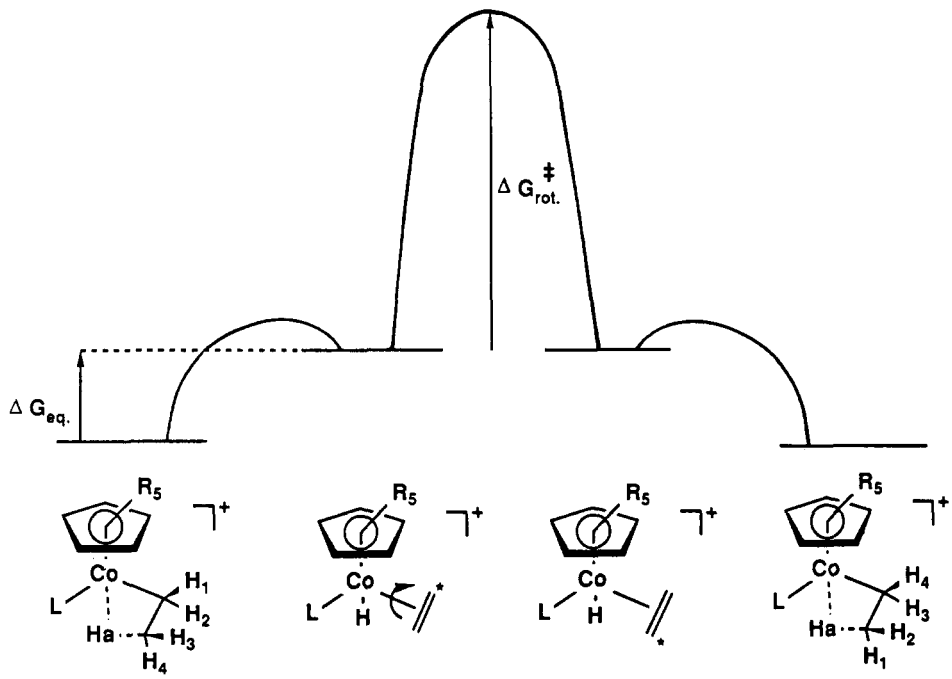

Chart I. Assuming the 16-electron species 8 lies close to the transition state for methyl rotation (i.e., δ is small), the actual barrier for inversion at cobalt in the 16-electron species 8 must be quite low i.e., 2.5 + δ kcal/mol.[19] For both **4a** and **10** the activation barrier for process III is only slightly (ca. 2.5 kcal/mol) higher than the barrier for methyl rotation (process I). If it is assumed that (a) the inversion barrier requires the intermediacy of the 16-electron species 8 and (b) methyl rotation occurs by an "in place" mechanism,[18] then the barrier to formation of the 16-electron species 8 can be at most 2.5 kcal/mol more than the "in place" rotational barrier.

The free energy diagram that applies to process II is shown in Chart II and indicates that $\Delta G^{\ddagger}_{obsd} = \Delta G_{equil} + \Delta G^{\ddagger}_{rot}$. Model compounds suggest that $\Delta G^{\ddagger}_{rot}$ should be substantial, probably in the range of 10–15 kcal/mol. For example, the ethylene rotational barrier in the Co(III) complex $Cp^*Co(Me)_2(C_2H_4)$ is 12.4 kcal/mol[20] while the barrier for C_2H_4 rotation in $Cp^*(P(OMe)_3)Rh(C_2H_4)(H)^+$ is 10.2 kcal/mol.[21] If barriers of this magnitude apply to **4a,b** and **5a,b**, then ΔG_{eq}, the energy difference between classical and agostic structures, must be quite small. It has been shown that the energy difference between the agostic species $Cp^*Co(C_2H_4)(CH_2CH_2\text{-}\mu\text{-}H)^+$ and its classical hydride analogue is a maximum of 7.2 kcal/mol.[8]

Spectroscopic Analysis of $Cp^*(P(OMe)_3)Co\text{-}C_2H_3CH_3\text{-}\mu\text{-}H^+$. Protonation of the propene complex **13** results in formation of three isomeric bridged structures, **14**, **15**, and **16**, shown in Scheme II. The detailed NMR analysis and methods of chemical shift assignments in this system are quite complex and details are summarized in the Experimental Section. Key ^1H and ^{13}C data are listed below each structure. The upfield region of the ^1H NMR

(19) Calculations suggest that the 16-electron fragment $CpMn(CO)_2$ analogous to 8 has a pyramidal geometry with a very low barrier to inversion: Hofmann, P. *Angew. Chem., Int. Ed. Engl.* **1977**, *16*, 536.

(20) Pardy, R. B. A. *J. Organomet. Chem.* **1981**, *216*, C29.
(21) Lincoln, D.; Brookhart, M., unpublished results.

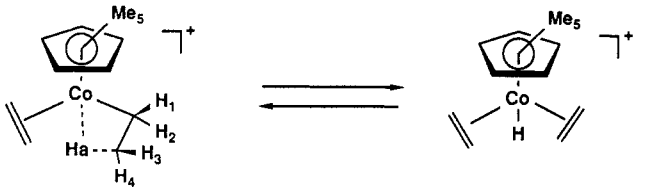

11 12

spectrum of the equilibrium mixture of β-CH_3-**14**, β-CH_3-**15**, and α-CH_3-**16** is shown in Figure 1 and clearly shows three separate H_a signals for the three isomers. Through extensive decoupling and spin saturation transfer NMR experiments nearly complete assignment of all resonances was possible; details are contained in the Experimental Section.

There are two significant features regarding this system that should be noted. First, this set of methyl-substituted isomers has provided an assignment of the homologous sets of alkyl-substituted bridged isomers formed as **4b** undergoes polymerization with ethylene:[12]

4 b **17a,b,c**

a R_1 = alkyl, R_2 = H, R_3 = H

b R_1 = H, R_2 = alkyl, R_3 = H

c R_1 = H, R_2 = H, R_3 = alkyl

alkyl = n-C_2H_5, n-C_4H_9, n-C_6H_{13}, etc.

Second, the unusual values of J_{CH_a}, J_{PH_a}, and $\delta(^{13}C_\beta)$ in major isomer **14** yield additional structural information. The J_{CH_a} of 38.5 Hz is much lower than the "normal" agostic J_{CH_a}'s in this system (60–63 Hz) but too large for a classical hydride. Similarly, the J_{PH_a} has increased substantially (39 Hz) but is less than expected for a classical, terminal hydride (80 Hz, see above). The $\delta(^{13}C)$ shift of C_β is substantially downfield from $\delta(C_\beta)$ of isomers **15** and **16** (also **4** and **5**) and indicates more olefinic character for this C_β carbon. There are two possible interpretations of this data. (1) The methyl group perturbs the relative stabilities of classical and bridged structures such that they are now approximately equi-energetic with a low barrier (<6 kcal/mol) between them and they rapidly equilibrate on an NMR time scale. The observed J_{CH_a}, J_{PH_a}, and $\delta(^{13}C_\beta)$ values are weighted average values for the classical and bridged structures:[22]

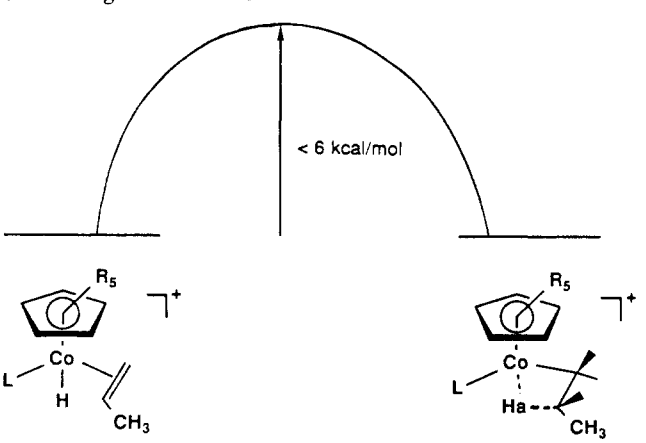

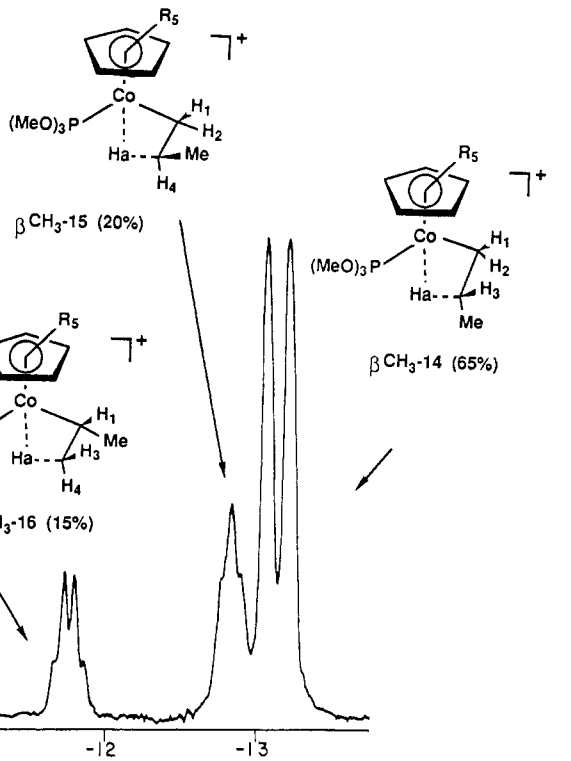

Figure 1. ^1H NMR of upfield region of spectrum of equilibrium mixture of isomers **14**–**16**.

This model assumes a well-defined, invariant structure for the Co···H···C bonds in these agostic species. Alternatively, (2) there is a very flat potential connecting a "normal" agostic structure and the terminal hydride **9** and the minimum energy structure can be significantly altered by substituents at the β-carbon of the "ethylene" unit.

Currently, we favor the latter explanation, but with little evidence. It seems unlikely that there would be a significant barrier accompanying rather minor changes in the C_β–H_a and Co–C_β bond lengths. Furthermore, no temperature dependence of the chemical shift of H_a or C_β nor of J_{PH_a} is noted (as may be expected for a double minimum), but the temperature range is narrow and limited due to dynamic processes above –60 °C.[23] Spencer's recent work[15] shows that systematic variation of the properties of the phosphine chelate ligand in **18** results in a systematic

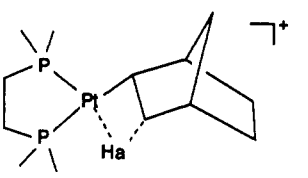

18

variation of J_{Pt-H} which is in accord with a flat potential in which the minimum energy structure is quite sensitive to the nature of the metal ligands. However, even in this case a double minimum system with variation in K_{eq} cannot be ruled out. Regardless of which alternative applies, it is reasonable to conclude that in these Co(III) systems there is a very small energy difference between

(22) If we assume J_{CH} = 0 and J_{PH} = 80 Hz for a terminal hydride structure and J_{CH} = 60 Hz and J_{PH} = 12 Hz for an agostic structure, then the weighted average values suggest an equilibrium ratio of ca. 2:1 agostic:terminal in isomer **14**.

(23) The chemical shift of C_β of **14** is invariant from –60 to –110 °C.

Scheme II

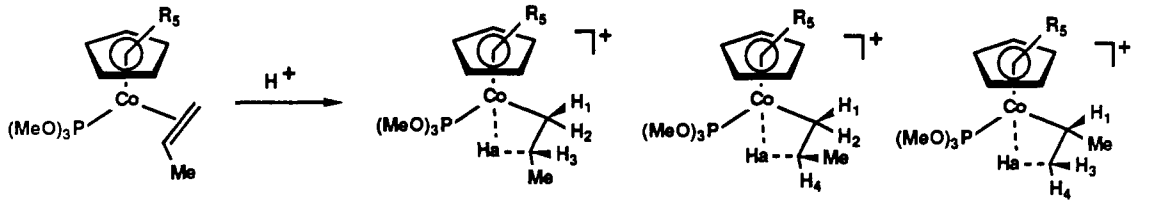

13	β CH_3-14 (65%)	β CH_3-15 (20%)	α CH_3-16 (15%)	
δH_a =	-13.2	-12.8	-11.8	(ppm)
$\delta 13_{C_\beta}$ =	29.9	8.7	-0.2	(ppm)
$J_{C_\beta H_a}$ =	38.5	Masked	61	(Hz)
J_{PH} =	39	<17	<18	(Hz)

terminal hydride and agostic structures. We are currently examining other systems that will yield information regarding energy differences between classical and agostic systems and the nature of the potential connecting the two forms.

Experimental Section

General Information. All complexes were manipulated under an atmosphere of dry, oxygen free nitrogen within a Vacuum Atmospheres drybox or on a standard Schlenk line. All solvents and reagents were dry and degassed. ^1H and ^{13}C NMR spectra were recorded on either a Varian XL-400, Bruker WM-200, or a Bruker WM-250 spectrometer. All precursor ethylene complexes were prepared by using published procedures.[24,25] Analysis of **13** was performed by Galbraith on a sample which was shipped at −78 °C.

Preparation of $Co(C_5Me_5)(P(OMe)_3)(C_2H_3CH_3)$ (13). An eightfold excess of 1% sodium–mercury amalgam (1.64 g of Na/164 g of Hg) in THF (150 mL) was saturated for 15 min with propylene introduced via a syringe needle. A solution of $[(C_5Me_5)Co(I_2)]_2$ (4 g, 0.0045 mol) in THF (100 mL) and under nitrogen was added to the THF/amalgam/olefin mixture by means of a cannula. The mixture was stirred vigorously for 1 h while the olefin purge was maintained. After a few minutes the solution changed from a green color to dark red. The solution was filtered through celite to remove solid NaI. $P(OMe)_3$ (0.43 mL, 0.60 equiv to reduce formation of the bis(phosphite) complex) was then added by syringe, and the solution was left to stir at 25 °C for 20 h while under N_2. Solvent was removed under vacuum, and the resulting dark red oily solids were extracted with a minimum (50 mL) amount of 2-methylbutane. This solution was filtered through Celite, and the solvent volume was reduced for crystallization (10 mL) at −78 °C for 40 h. Red crystals were isolated by decantation of the supernatant at −78 °C and washed several times with 2-methylbutane. Residual solvent was removed at 25 °C under vacuum to leave red crystals (1.30 g, 40% yield). The complex could be stored at −40 °C, but noticable decomposition occurs at 25 °C over 3–5 h. ^1H and ^{13}C NMR spectroscopy shows the presence of two isomers in a ca. 5.4:1 ratio. ^1H NMR (25 °C, C_6D_6): major isomer, δ 1.35–1.60 (complex, $=CH_2$), 1.58 (d, 6.4 Hz, CH_3), 1.69 (d, J_{PH} = 1.6 Hz, C_5Me_5), 1.96 (m, =CH), 3.27 (d, J_{PH} = 11.6 Hz, $P(OMe)_3$); minor isomer, 1.78 (d, J_{PH} = 1.9 Hz, C_5Me_5), 3.29 (d, J_{PH} = 11.2 Hz, $P(OMe)_3$). ^{13}C NMR (25 °C, C_6D_6): major isomer, δ 9.77 (q, 126 Hz, C_5Me_5), 21.7 (q, 126 Hz, $=CHCH_3$), 35.6 (t, 147 Hz, $CH=CH_2$), 45.9 (d, 142 Hz, $CH=$), 49.2 (q, 147 Hz, $P(OMe)_3$), 91.4 (s, C_5Me_5); minor isomer, δ 10.6 (q, 126 Hz, C_5Me_5), 20.9 (q, 126 Hz, $=CHCH_3$), 33.7 (d, 147 Hz, $CH=CH_2$), 44.2 (d, 142 Hz, $CH=$), 49.7 (q, 147 Hz, $P(OMe)_3$). Anal. Calcd for $C_{16}H_{30}O_3PCo$ (360.32): C, 53.33; H, 8.39. Found: C, 52.85; H, 8.50.

Generation and NMR Spectroscopic Characterizations of Agostic Complexes 4a,b and 5a,b. Typical Procedure. $Co(C_5H_5)(PMe_3)(C_2H_4\text{-}\mu\text{-}H)^+$ (5a). $Co(C_5H_5)(PMe_3)(C_2H_4)$ (0.10 mg, 0.044 mmol) was weighed out in the drybox and dissolved in 0.75 mL of CD_2Cl_2 in an NMR tube blanketed with nitrogen and equipped with a side arm. The solution was cooled to −78 °C while under nitrogen on a standard vacuum line. $HBF_4\cdot Me_2O$ complex (1.3 equiv. 0.057 mmol) was syringed into the solution. The solution was then stirred while the temperature was allowed to rise to approximately −30 °C. Once the $HBF_4\cdot Me_2O$ complex completely dissolved, the resulting deep red solution was frozen in liquid nitrogen and sealed under vacuum. The sample was warmed to −80 °C and introduced into a −70 °C precooled probe for analysis. ^{13}C NMR samples were prepared in a similar fashion employing 30 mg of the neutral precursor and 1.3 equiv of $HBF_4\cdot Me_2O$. **5a**: ^1H NMR (−70 °C, CD_2Cl_2) δ −13.0 (H_a), −0.8 (m, H_3 or H_4), 0.25 (m, H_3 or H_4), 1.5 (m, H_1 or H_2), 4.0 (masked by Me_2O, H_1 or H_2), 5.05 (s, C_5H_5), 1.0 (d, 11.8 Hz, PMe_3); ^{13}C NMR (−70 °C, CD_2Cl_2) δ −9.6 (td, J_{CH} = 152, 60 Hz, C_β), 20.4 (t, J_{CH} = 155.7 Hz, C_α), 15.2 (dq, J_{PC} = 32.3 Hz, J_{CH} = 130 Hz, PMe_3), 85.6 (dd, J_{PC} = 6.6 Hz, J_{CH} = 176 Hz, C_5H_5).

$Co(C_5H_5)(POMe_3)(C_2H_4\text{-}\mu\text{-}H)^+$ (5b). The NMR samples were prepared as for **5a**, employing 10 mg of neutral precursor for the ^1H NMR sample and 30 mg for the ^{13}C NMR sample. **5b**: ^1H NMR (−70 °C, CD_2Cl_2) δ −12.4 (H_a), −0.7 (m, H_3 or H_4), 0.2 (m, H_3 or H_4), 1.8 (m, H_1 or H_2), 4.0 (masked by Me_2O, H_1 or H_2), 5.07 (s, C_5H_5), 3.45 (d, 11.9 Hz, $P(OMe)_3$); ^{13}C NMR (−70 °C, CD_2Cl_2) δ −9.2 (td, J_{CH} = 154, 61 Hz, C_β), 86.4 (d, J_{CH} = 176 Hz, C_5H_5), 22.4 (t, J_{CH} = 154 Hz, C_α), 53.0 (q, J_{CH} = 140 Hz, $P(OMe)_3$).

$Co(C_5Me_5)(PMe_3)(C_2H_4\text{-}\mu\text{-}H)^+$ (4a). The NMR samples were prepared as for **5a** by using 10 mg of ethylene complex for the ^1H NMR sample and 30 mg for the ^{13}C NMR sample. **4a**: ^1H NMR (−70 °C, CD_2Cl_2) δ −12.6 (H_a), −0.42 (m, H_3 or H_4), −0.18 (m, H_3 or H_4), 1.23 (m, H_1 or H_2), 2.7 (m, H_1 or H_2), 1.7 (s, C_5Me_5), 1.1 (d, 9.0 Hz, PMe_3); ^{13}C NMR (−70 °C, CD_2Cl_2) δ −4.7 (td, J_{CH} = 151, 63 Hz, C_β), 25.8 (t, J_{CH} = 157.4 Hz, C_α), 95.1 (s, C_5Me_5), 9.2 (q, J_{CH} = 129 Hz, C_5Me_5), 13.1 (dq, J_{CP} = 30.7 Hz, J_{CH} = 130 Hz, PMe_3).

$Co(C_5Me_5)(P(OMe)_3)(C_2H_4\text{-}\mu\text{-}H)^+$ (4b). The NMR samples were prepared as for **5a** by using 10 mg of ethylene complex for the ^1H NMR sample and 30 mg for the ^{13}C NMR sample. **4b**: ^1H NMR (−70 °C, CD_2Cl_2) δ −12.1 (H_a), −0.3 (m, H_3 or H_4), −0.2 (m, H_3 or H_4), 1.9 (m, H_1 or H_2), 2.5 (m, H_1 or H_2), 1.7 (s, C_5Me_5), 3.5 (d, J_{PH} = 10 Hz, $P(OMe)_3$); ^{13}C NMR (−90 °C, CD_2Cl_2) δ −5.8 (td, J_{CH} = 152, 61 Hz, C_β), 8.3 (q, 129 Hz, C_5Me_5), 26.5 (t, 160

(24) Beevor, R. G.; Frith, S. A.; Spencer, J. L. *J. Organomet. Chem.* **1981**, *221*, C25.
(25) Hofmann, L.; Werner, H. *J. Organomet. Chem.* **1985**, *289*, 141.

Hz, C_α), 52.0 (q, 147 Hz, OMe), 96.8 (s, C_5Me_5).

$Co(C_5Me_5)(P(OMe)_3)(C_2H_3CH_3$-$\mu$-$H)^+$ (14–16). The NMR samples were prepared as for **4a**: 10 mg of propylene complex **13** for the ^1H NMR sample and 30 mg for the ^{13}C NMR sample.

$(C_5Me_5)(P(OMe)_3)(C_3H_7)CoBF_4$: ^1H and ^{13}C NMR Characterization. β-CH_3-**14**: ^1H NMR (−70 °C, CD_2Cl_2) δ −13.2 (d, J_{PH} 39 Hz, H_a), 1.4 (br m, H_3), 1.9 (br dt, H_2), 2.8 (br d, 6 Hz, H_1); ^{13}C NMR (−70 °C, CD_2Cl_2) δ 8.40 (q, 128 Hz, C_5Me_5), 15.0 (q, 122 Hz, CMe), 29.9 (dd, J_{CH} = 148 Hz, 38.5 Hz, C_β), 39.0 (td, 156 Hz, J_{CP} = 9 Hz, C_α), 52.0 (J_{CP} = 4 Hz, J_{CH} masked by solvent resonances in coupled spectrum, OMe), 97.9 (s, C_5Me_5).

β-CH_3-**15**: ^1H NMR (−70 °C, CD_2Cl_2) δ −12.8 (br t, 17 Hz, H_a), 0.1 (br m, H_4), 2.2 (br d, 10 Hz, H_1), 2.3 (br d, 12 Hz, H_2); ^{13}C NMR (−70 °C, CD_2Cl_2) δ 8.7 (masked by C_5Me_5 signals in coupled spectrum, C_β), 9.0 (q, 128 Hz, C_5Me_5), 13.3 (q, 122 Hz, CMe), 31.1 (td, 148 Hz, J_{CP} = 12 Hz, C_α), 52.5 (masked by solvent signals in coupled spectrum, OMe), 96.7 (s, C_5Me_5).

α-CH_3-**16**: ^1H NMR (−70 °C, CD_2Cl_2) δ −11.8 (br q, 18 Hz, H_a), −0.2, −0.3 (br m, H_3 and H_4), 2.1 (br dd, 18 Hz, 7 Hz, H_1); ^{13}C NMR (−70 °C, CD_2Cl_2) δ −0.2 (td, J_{CH} = 150, 61 Hz, C_β), 8.2 (q, 128 Hz, C_5Me_5), 15.7 (q, 122 Hz, C_{Me}), 44.5 (dd, 151 Hz, J_{CP} = 9 Hz, C_α), 53.4 (masked by solvent signals in coupled spectrum, OMe), 97.8 (s, C_5Me_5).

Assignments of Isomers β-CH_3-14, β-CH_3-15, and α-CH_3-16. To assign isomers, spin saturation transfer experiments were used in conjunction with standard line broadening experiments. The β-methyl-substituted isomers β-CH_3-**14** and β-CH_3-**15** can interconvert by dynamic process I which occurs with the lowest activation barrier ($\Delta G^\ddagger$ = ca. 11 kcal/mol) and causes line broadening above ca. −50 °C. The β-isomers can interconvert with the α-isomer(s) *only* at higher temperature via dynamic process II ($\Delta G^\ddagger$ = ca. 14 kcal/mol). The dynamic properties allow differentiation of α-isomers from β-isomers, and, in addition, spin saturation transfer experiments allow specific chemical shift assignments to be made. Key ^1H and ^{13}C NMR experiments are outlined below.

Rotation about the C_α–C_β bond (dynamic process I) interconverts isomers β-CH_3-**14** and β-CH_3-**15** and leads to substantial broadening above −40 °C of ^{13}C resonances at δ 31.0 and 39.0 (C_α's), δ 29.9 and 8.7 (C_β's), and δ 15.0 and 13.3 (CH–CH_3's). The remaining signals that do not broaden at this temperature were assigned to isomer α-CH_3-**16**.

At −48 °C ^1H spin saturation transfer established interchange of the following sites in isomers β-CH_3-**14** and β-CH_3-**15** due to dynamic process I (assignments are given in parentheses): δ −13.2 exchanges with δ +0.1 (H_a of isomer **14** and H_4 of isomer **15**); δ 1.4 exchanges with δ −12.8 (H_3 of isomer **14** and H_a of isomer **15**); δ 1.9 exchanges with δ 2.3 (H_2 of isomer **14** and H_2 of isomer **15**); δ 2.8 exhanges with δ 2.2 (H_1 of isomer 14 and H_1 of isomer **15**). (The last two sets of assignments may be reversed). The remaining signals did not exhibit spin saturation transfer with either isomer β-CH_3-**14** or β-CH_3-**15** and thus were assigned to the α-isomer α-CH_3-**16**.

The ratios of the three isomers were determined by integration of the H_a resonances at δ −13.2, −12.8, and −11.8. Although the two major isomers are clearly β-methyl isomers, the assignments of the major β-isomer to structure β-CH_3-**14** is arbitrary and is based solely on steric considerations. Likewise, assignment of the sole α-methyl isomer observed to structure α-CH_3-**16** (as opposed to its epimer) is also arbitrary and is based on steric considerations.

Acknowledgment is made to the National Science Foundation (CHE-8705534) and the National Institutes of Health (GM-23938) for support of this research.

Registry No. **4a** (BF_4), 91310-54-2; **4b** (BF_4), 94669-93-9; **5a** (BF_4), 119567-82-7; **5b** (BF_4), 119567-84-9; **13** (isomer 1), 119617-95-7; **13** (isomer 2), 119617-96-8; **14** (BF_4), 119617-98-0; **15** (BF_4), 119618-00-7; **16** (BF_4), 119567-86-1; $[(C_5Me_5)Co(I_2)]_2$, 72339-52-7; $Co(C_5H_5)(PMe_3)(C_2H_4)$, 99898-04-1; $Co(C_5H_5)(P(OMe)_3)(C_2H_4)$, 99898-05-2; $Co(C_5Me_5)(PMe_3)(C_2H_4)$, 91310-48-4; $Co(C_5Me_5)(P(OMe)_3)(C_5H_4)$, 94645-00-8; propylene, 115-07-1.

Supplementary Material Available: Figure S1, variable-temperature ^1H NMR spectra illustrating the methyl rotation process in $Cp^*Co(P(OMe)_3)(C_2H_4$-μ-$H)^+$, Figure S2, variable-temperature ^{13}C NMR illustrating the olefin rotation process in $Cp^*Co(P(OMe)_3)(C_2H_4$-μ-$H)^+$, and Figure S3, ^1H NMR decoupling experiments on $Cp^*Co(P(OMe)_3)(C_2H_4$-μ-$H)^+$ showing the coupling relationships between H_a and H_1, H_2, H_3, H_4 (3 pages). Ordering information is given on any current masthead page.